Giant magnetic moment in an anomalous ferromagnetic insulator: Co-doped ZnO

C. Song, K. W. Geng, F. Zeng, X. B. Wang, Y. X. Shen, and F. Pan*
Laboratory of Advanced Materials, Department of Materials Science and Engineering, Tsinghua University, Beijing 100084, People's Republic of China

Y. N. Xie, T. Liu, H. T. Zhou, and Z. Fan
BSRF Beijing Synchrotron Radiation Facility, Chinese Academy of Science, Beijing 100039, People's Republic of China
(Received 24 September 2005; revised manuscript received 21 November 2005; published 12 January 2006)

Ferromagnetic insulators that exhibit strong ferromagnetism at the atomic level are believed to be suitable for magnetic dielectric barriers in spintronic devices and solid-state qubits in quantum computing. Here a giant magnetic moment of $6.1\mu_B$/Co and a high Curie temperature T_C of 790 K are observed in (4 at. %) Co-doped ZnO films, which is not carrier mediated, but co-exists with the dielectric state. Direct current reactive magnetron co-sputtering is used to grow $Zn_{0.96}Co_{0.04}O$ dilute magnetic insulator on $LiNbO_3$ (104) substrates at considerably low growth temperature (~200 °C), which is significant for complementary metal oxide semiconductor technology. X-ray photoelectron spectroscopy and x-ray-absorption spectroscopy reveal a solid solution of cobalt in ZnO, where Co is in the 2+ state substituting for Zn. A supercoupling mechanism in terms of bound magnetic polarons is proposed to discuss the ferromagnetism in the dielectric ground state of Co:ZnO, which would lead to different consideration for the origin of giant magnetic moment and high-temperature ferromagnetism in transition-metal doped oxides.

DOI: 10.1103/PhysRevB.73.024405 PACS number(s): 75.30.−m, 72.80.Sk, 75.70.−i

I. INTRODUCTION

Spin ordering in tunnel junctions made of barriers that are diluted ferromagnetic insulators (DMIs) such as EuS has interested researchers since observation by Esaki of large magnetic-field effect.[1] The topic has attracted renewed interest because recent experiments have revealed that the transverse and longitudinal relaxation times for electron spins in insulating quantum dots are in the nanosecond regime and offer promise for their utilization as computing elements in quantum electronics.[2,3] However, EuS failed in the practical sense, because their ferromagnetic transition temperatures were much lower than room temperature with little hope of great improvement.[4] Thus the requirement for room-temperature solid-state qubits based on spin filter effect can become a reality only with the advent of ferromagnetic insulators at room temperature.

Room-temperature ferromagnetism has been recently demonstrated in highly insulating transition-metal doped TiO_2 anatase, such as $Co:TiO_2$,[5,6] $Cr:TiO_2$ (Ref. 7) with magnetic moment of $1.1\mu_B$/Co and $0.6\mu_B$/Cr, respectively. On the other hand, two mechanisms, bound magnetic polarons as discussed by Sarma *et al.*[8] for highly resistive GaMnAs and *F*-center-mediated exchange as recently proposed by Coey *et al.*,[9] have been reported to understand the ferromagnetism in DMI for the absence of carrier-mediated exchange. Unfortunately, all these DMIs exhibit weak ferromagnetism and low T_C (below 350 K), reducing their practical usefulness.[10] It is hence of vital importance to design new insulators that exhibit strong ferromagnetism at the atomic level.

ZnO has been selected as a host of DMIs in this work for two reasons. First, structures and properties of doped ZnO have interested researchers in the last few years since predictions by Dietl *et al.*[11] of T_C far in excess of 300 K. In fact, ZnO continues to attract attention for short-wavelength emission, transparent electronics, and spintronic devices because of its large band gap (3.37 eV), large excition binding energy (60 meV), and the ability to achieve room-temperature ferromagnetism by doping with transition metals.[12–19] However, all these doped ZnO films prepared by pulsed-laser deposition[14–17] and metalorganic chemical vapor deposition[18] are either conducting or semiconducting. Second, in general, cobalt is seen to be in the 2+ valence state in diluted magnetic semiconductors (DMSs), which is equal to that of Zn^{2+}. The *F*-center model can be discounted at this time for no O vacancies to maintain charge neutrality,[9] which challenges our understanding of magnetism of DMIs.

In this paper, we report the magnetic properties of dilute (4 at. %) cobalt doping ZnO on $LiNbO_3$ (104) prepared by reactive magnetron co-sputtering, which is low-temperature processing with high preparation efficiency. A giant magnetic moment $6.1\mu_B$/Co in Co:ZnO films with high-temperature ferromagnetism are obtained.

II. EXPERIMENT

$Zn_{0.96}Co_{0.04}O$ films were deposited on (104) $LiNbO_3$ (LNO) single-crystal substrates by direct current reactive magnetron co-sputtering. The relative sputtering area of Co chips was adjusted to control the Co composition in the deposited Co-doped ZnO film, which were attached on a Zn target (99.999% purity). The base pressure of the sputter deposition chamber was 4×10^{-6} Torr, and the working pressure was a mixture of argon 2.5×10^{-3} Torr and oxygen at 4.2×10^{-3} Torr. The deposition rate is 0.05 nm/s and the substrate temperature during deposition was ~200 °C. The film structure and crystalline quality were characterized by x-ray diffraction (XRD). High-resolution transmission elec-

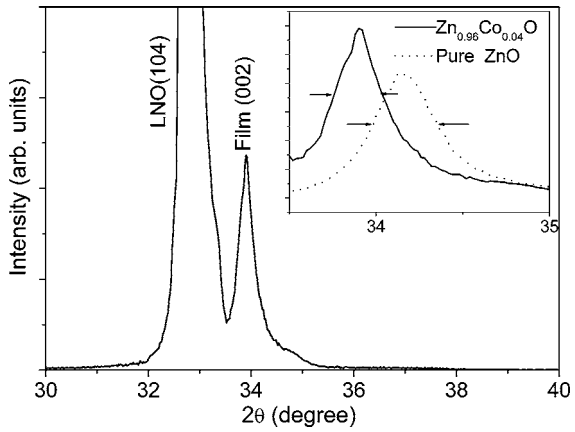

FIG. 1. XRD spectra of the Co-doped ZnO. The inset of the figure shows a comparison of (002) reflections of Co-doped ZnO (solid line) and the pure ZnO (dotted line).

tron microscopy (HRTEM) imaging, selected area electron diffraction (SAD), energy-dispersive x-ray spectroscopy (EDS), and electron energy loss spectroscopy (EELS) were used to study the interface bonding and structural characteristics of the films. X-ray photoelectron spectroscopy (XPS) spectra were characterized to verify the Co composition of films for bulk analysis and the existence form of cobalt in the $Zn_{0.96}Co_{0.04}O$ films. X-ray-absorption near-edge spectrum (XANES) at the Co *K*-edge was measured to determine the valence state and local geometry of the Co dopant in the ZnO lattice. Magnetization studies were carried out using a superconducting quantum interference device (SQUID) magnetometer (MPMS, Quantum Design) in the temperature range 5–350 K. High-temperature magnetization ($300 < T < 800$ K) was recorded using a vibrating sample magnetometer (VSM). Induced-coupled-plasma (ICP) atomic emission spectrums were used to determine the Co contents in the samples after measuring the magnetic properties. The average magnetic moment per Co ion was then calculated. The relative dielectric constant (ε_r) and leakage electricity of patterned Co-doped ZnO films were performed on a TF Analyser 2000.

III. RESULTS AND DISCUSSIONS

The lattice dismatch of ZnO ($a=3.245$ Å, $c=5.207$ Å, hexagonal) to the $LiNbO_3$ (LNO) ($a=5.149$ Å, $c=13.862$ Å, rhombohedral) substrate results in preferred orientation of polycrystalline Co:ZnO film instead of epitaxial growth, as depicted in typical XRD measurement (Fig. 1). It clearly shows *c*-axis orientations with (002) peaks (measured *c*-lattice parameter $c=5.288$ Å). The inset of Fig. 1 compares the peaks for Co:ZnO and pure ZnO films. Interestingly, a comparison of the full width at half maximum (FWHM) values of (002) peak intensities of Co-doped and the pure ZnO films show an improvement in crystallinity with doping by a 0.12° decrease in the FWHM value. Also visible in the inset is the relative shift of the (002) peak to a lower angle for the Co:ZnO, indicating Co incorporation into the wurtzite lattice. Thus Co doping has a stabilization effect on the phase

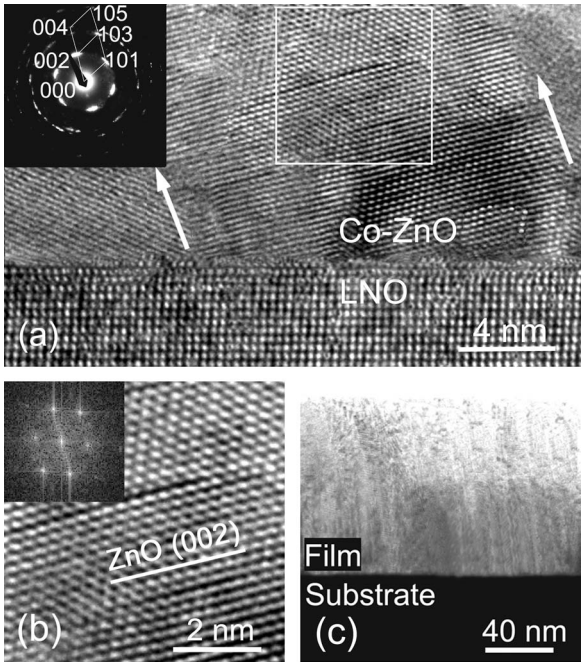

FIG. 2. (a) The high-resolution TEM of $Zn_{0.96}Co_{0.04}O/LNO$ cross section. The inset is the SAD pattern of $Zn_{0.96}Co_{0.04}O$ films. (b) Fourier transform (FFT) along the [002] zone axis corresponding to the □-like area in (a). (c) Low magnification image of the cross-section specimens.

of ZnO in its (002) preferred orientation film form at significantly lower growth temperature of 200 °C. All films are single phase with no evidence of secondary phases within the sensitivity of XRD measurements.

The typical cross-sectional HRTEM image and selected area electron diffraction (SAD) of the $Zn_{0.96}Co_{0.04}O/LNO$ films are shown in Fig. 2(a). There was no observation for the presence of Co metal (above 5 at. %) or Co-rich wurtzite clusters in the overall of films. EDS data taken at a number of locations throughout the specimens reveal a solid solution of Co dissolved in ZnO, with Co concentrations ranging from ~3.8–4.7 at. % incorporated into the lattice. The inset of Fig. 2(a) is a SAD pattern confirming Co:ZnO films grown onto the LNO substrate behave with preferred orientation. A representative (002) crystal grain is marked by two arrows in Fig. 2(a). That is, the area between the two arrows is a ~16-nm diameter pillarlike grain. The corresponding fast Fourier transform (FFT) along the [002] zone axis is displayed in Fig. 2(b). Low magnification image of the cross-section specimens in Fig. 2(c) reveals the uniform thickness (~120 nm) and columnar structure of the films.

The film composition as a function of thickness was characterized using XPS depth profiling with the sputtering rate of 6 nm/min. Figure 3(a) shows a plot of Zn, Co, O, Li, and Nb atoms normalized to the total atoms as a function of sputter depth for (~4 at. %) Co:ZnO films. The film-substrate interface is marked by the rapid increase of the Li and Nb atomic concentration at approximately 120 nm, which suggests that the thickness of Co:ZnO films is ~120 nm. It is found that the profiles are very flat, indicating that the Co and Zn are uniformly distributed throughout the

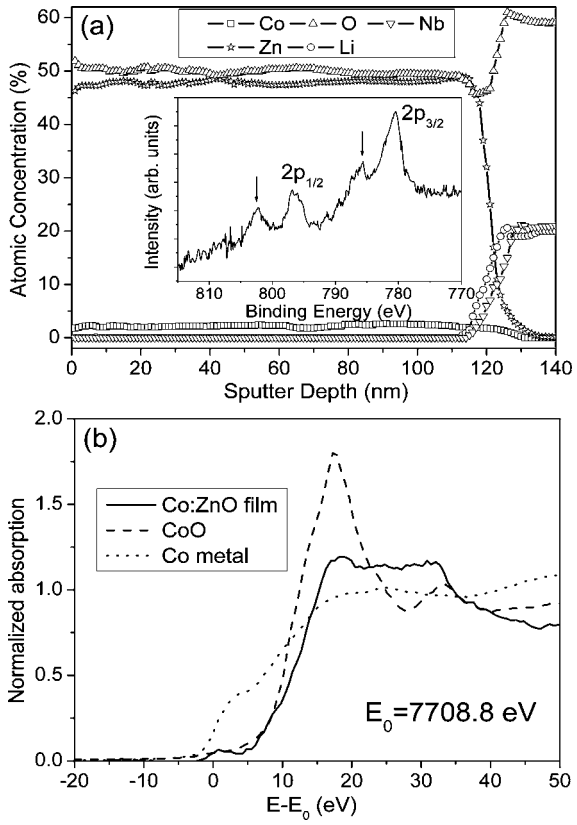

FIG. 3. (a) Zn, Co, O, Li, and Nb XPS depth profiles for $Zn_{0.96}Co_{0.04}O$/LNO films. Inset: XPS spectra at 50-nm depth of films. Two arrows indicate the shake-up satellites. (b) Co *K*-edge XANES spectra for (4 at. %) Co:ZnO film with reference samples: Co metal and CoO.

film and that very little, if any, segregation exists at the surface. XPS was also used to characterize the charge state of Co ions in the films. This attempt is made to understand the magnetic and electrical properties of the DMI. The inset of Fig. 3(a) highlights the Co 2*p* core-level photoemission spectrum from a depth of 50 nm of $Zn_{0.96}Co_{0.04}O$ film. Comparison of the shaped and positions of the primary and satellite peaks shows that there is a good fit between the $Zn_{0.96}Co_{0.04}O$ films and the Co^{2+} standard.[18] Thus Co is in 2+ valence state in Co:ZnO films.

It is difficult to confirm the Co^{2+} state in XPS charge state, which may come from CoO clusters and Co^{2+} ions incorporating into the wurtzite lattice at Zn^{2+} ion sites. Hence we have employed Co *K*-edge XANES to obtain the valence state and local geometry of Co dopant in the lattice, because Co *K*-edge XANES has the advantage of sensitivity to submonolayer equivalent concentrations of Co and a large chemical shift between the onset of absorption for Co^0 and Co^{2+}, which is much more sensitive to local structural than Co *L*-edge XANES.[20] Co *K*-edge XANES spectra from (4 at. %) Co-doped ZnO and various reference materials (Co metal, CoO) are shown in Fig. 3(b). The plateau at $E-E_0=3$ eV ($E_0=7708.8$ eV) in the Co metal spectrum is unique to Co^0 and can be effectively used to determine the presence of Co metal. This plateau is different from the small feature observed at $E-E_0=0$ eV of Co:ZnO spectrum,

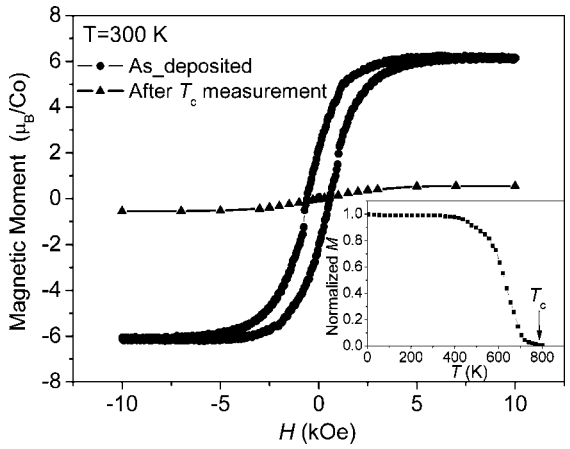

FIG. 4. *M-H* loop at 300 K of as-deposited $Zn_{0.96}Co_{0.04}O$ films (solid circle). The inset is the normalized (M/M_{5K}) *M-T* curve. The hysteresis loops measured at 300 K after T_C measurement is also plotted (solid triangle).

which is due to a 1*s* to 3*d* weak pre-edge resonance that becomes partially dipole allowed when Co is coordinated to O ligands and Co 3*d*/O 2*p* mixing occurs in low-lying conduction-band states.[20] Therefore it is clear that the plateau near threshold associated with Co^0 is absent in spectra for Co:ZnO, as well as in spectra for CoO. On the other hand, the absorption edge of Co metal is poor match to the Co:ZnO films due to the much lower threshold energy corresponding to the Co^0 state. Thus there is no detectable Co^0 in (4 at. %) Co-doped ZnO film.

The obvious difference of the XANES spectra between Co:ZnO film and CoO indicates that in Co:ZnO film Co incorporate into the wurtzite lattice, i.e., the Zn site in wurtzite, instead of in the CoO form. Similar results have been obtained by Griffin *et al.*[5] in the $Co:TiO_2/LaAlO_3$ system, the closer match of XANES spectrum of the sputtered $Co:TiO_2$ film to $CoTiO_3$ than to CoO is indicative of the distorted octahedral coordination of the Co atom in the lattice (i.e., the Ti site in anatase), whereas in CoO the Co site has an undistored octahedral configuration. In addition, the core peak of Co:ZnO films is significantly wider than that of metal Co and CoO. This may be attributed to the presence of tetrahedron coordination of the Co atom in the wurtzite lattice. Similarly to the shape of Mo *K*-edge XANES is broad corresponding to the tetrahedron coordination environment of the Mo atom in the oxidase.[21] Therefore from this comparison of Co *K*-edge spectrum it can be concluded that there is no evidence of Co metal throughout the film and Co^{2+} substitutes for Zn^{2+} in the lattice, since the ionic radii of four-coordinate Zn^{2+} and Co^{2+} (0.060 and 0.066 nm, respectively) differ by only 10% and Co^{2+} is very soluble in ZnO.[19]

Figure 4 reveals magnetic hysteresis loops (*M* vs *H*) at 300 K of $Zn_{0.96}Co_{0.04}O$ films, in which the average magnetic moment is obtained in terms of ferromagnetism measurement and ICP atomic-emission spectrums. It is useful to mention here that the hysteresis loops of the LNO substrate and holder are measured first with the largest magnetic moment about 2 orders of magnitude lower than that of Co:ZnO films, which are subtracted automatically by computer dur-

ing the measurement of $Zn_{0.96}Co_{0.04}O$ films in a magnetic field parallel to the film plane. Consequently, the hysteresis loops of Co:ZnO films are obtained. Apparently, the interference of the magnetization of the substrate and holder has a negligible effect on the measured value of the films and theprecision of the measured magnetic moment is to within less than 1%. The effective magnetron number in the samples is determined by ICP atomic emission spectrums after measuring the magnetic properties. The average magnetic moment per Co ion is then calculated. Taking into account an error of 5% in the ICP measurement, the total measured error is about 6%.[22] The most interesting result here is the reproducible giant magnetic moment of $6.1\mu_B$/Co ion, and room-temperature saturation magnetization (Ms) is attained at 3.5 kOe with a coercive filed (Hc) 610 Oe for as-deposited films. A similar giant magnetic moment of $7.2\mu_B$/Co was observed by Ogale *et al.* in a Co-doped SnO_2 DMS system.[23]

In general, the ferromagnet should have T_C above 500 K so that it can be used in a wide range of applications without temperature control.[10,24] The inset of Fig. 4 shows the ferromagnetic behavior of the film in the temperature range 5–350 K, as measured by SQUID magnetometer and the magnetization measured by vibrating sample magnetometer (VSM) for $300<T<800$ K. The T_C is seen to be about 790 K. As seen from this curve, the higher temperature (>300 K) magnetization shows a non-Brillouin-like behavior.[25] Such a behavior is theoretically expected in low-carrier density DMS ferromagnets and is suggested to be more typical of insulating DMS ferromagnets.[26] The hysteresis loops measured at 300 K after T_C measurement is also shown in Fig. 4, which means the Co:ZnO films are annealed under the pressure of 5×10^{-6} Torr to 800 K. From the figure, it is found that the giant magnetic moment is vanishing, which decreases to $\sim0.55\mu_B$/Co. This magnetic transition suggests that high-temperature process causes a rapid ferromagnetism decrease in Co:ZnO ferromagnetic insulator. This is consistent with the observed weak ferromagnetism in high-temperature processed samples in other studies.[16–18]

A series of (x at. %) Co:ZnO (x=1, 2, 3, 10, respectively) films were grown in the same way with (4 at. %) Co:ZnO. The magnetic moments are $1.2\mu_B$/Co ion, $1.3\mu_B$/Co ion, $2.4\mu_B$/Co ion, $0.4\mu_B$/Co ion for (x at. %) Co:ZnO (x=1, 2, 3, 10) films, respectively. Electrical resistance and Hall effect measurements could not be direct performed as a function of temperature on Co:ZnO thin films as the room-temperature resistance was quite high. The relative dielectric constants (ε_r) measured on patterned $Zn_{0.96}Co_{0.04}O$ films is 25, which is significantly greater than that of pure ZnO (ε_r=8). The leakage electricity of patterned $Zn_{0.96}Co_{0.04}O$ film is 5.56×10^{-2} mA/cm^2, and the corresponding resistivity is estimated to be $\sim10^9$ Ω cm. This high resistivity may attribute to wide band-gap character of ZnO (Ref. 12) and high oxygen partial pressure of 4.2×10^{-3} Torr in the film deposition process. Our results show good coincidence with other works[27,28] in which it was found that the gradual increase resistivity is accompanied by the increasing oxygen pressure, whereas doping ZnO, deposited in a high vacuum chamber, is the typical DMS reported previously.[12–19]

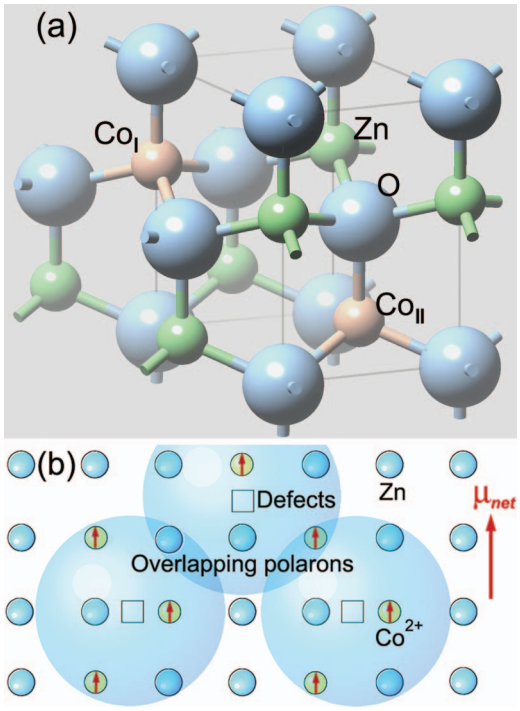

FIG. 5. (Color) (a) The lattice structure of (4 at. %) Co:ZnO. (b) Three-polaron subsystem is to represent supercoupling between polarons.

With interesting phenomena found in ferromagnetism measurement, research interest is in understanding of magnetism in solids. In magnetic insulators, the most common behavior is antiferromagnetism, where the susceptibility drops below the Néel temperature.[29] However, the room-temperature ferromagnetism with a giant magnetic moment $6.1\mu_B$/Co was unambiguously observed in (4 at. %) Co:ZnO ferromagnetic insulators. Several studies have been carried out on DMS, such as Co and Cr:SnO_2,[23,30] V-doped TiO_2 system,[31] to see very large magnetic moment of $7.2\mu_B$/Co, $6.0\mu_B$/Cr, $4.2\mu_B$/V, respectively, which are characterized by sp-d exchange between the s, p free carriers, and the d states of the transition-metal dopant. In the present case, the room-temperature resistance of $Zn_{0.96}Co_{0.04}O$ films was quite high with ε_r=25. This insulating nature is significant in that a magnetic coupling interaction other than carrier-mediated exchange is apparently operative. On the other hand, the charge valence of Co^{2+} is equal to that of Zn^{2+} in $Zn_{0.96}Co_{0.04}O$ films. Consequently, the F-center model is not suitable here for the absence of O vacancies. Moreover, conventional superexchange interactions cannot produce long-range magnetic order at concentrations of magnetic cations of a few percent, i.e., (4 at. %) Co:ZnO.

Based on the above analysis, a possible explanation for the intrinsic magnetism can be found invoking a supercoupling mechanism based on the bound magnetic polarons (BMP) model.[8,32] Figure 5(a) is the lattice structure of Co:ZnO, where Co^{2+} ions incorporating into the wurtzite lattice at Zn^{2+} ion sites on the basis of above experimental results. The highly nonequilibrium process of co-sputtering makes it possible that impurities (defects) in the doped film are located throughout the lattice at arbitrary distances with

respect to Co sites, which can play an important role in the system. An electron associated with a particular defect is confined in a hydrogenic orbital of radius $r_H=\varepsilon_r(m/m^*)a_0$ and $\gamma=\varepsilon_r(m/m^*)$, where ε_r is the dielectric constant, m is the electron mass, m^* is the effective mass of the donor electrons, and a_0 is the Bohr radius (0.53 Å). For (4 at. %) Co:ZnO, $m/m^*=0.28$,[24] $\varepsilon_r=25$. Hence high ε_r results in large r_H and γ, i.e., $r_H=3.7$ Å, $\gamma=7$. Taking into account a sufficiently large orbital radius, say $\gamma=7$, overlap between a hydrogenic electron and the cations within its orbit leads to ferromagnetic supercoupling between them, as shown in Fig. 5(b). The interaction between the hydrogenic electron and the cations is represented by a Heisenberg exchange Hamiltonian[29]

$$\hat{H}_{ij}=\sum_{ij} J_{ij}\hat{S}_i\hat{s}_j \tag{1}$$

where S is the spin of the Co^{2+} and s is the donor electron spin. The donors tend to form a BMP, coupling Co^{2+} within their orbits. The Hamiltonian of a two-polaron subsystem is given by Eq. (1), where donor electron spin index j takes only two values j_1 and j_2 corresponding to the two polarons under consideration.

It has been reported that the magnetic moment is enhanced as an orbital moment emerges in the nanoscale Fe cluster.[33] It may be possible that the contributions of both spin and orbital angular momenta co-exist in the present case which corresponds to the giant magnetic moment. More interestingly, using the Lande's g factor and the total angular momentum quantum number (J) of Co^{2+} in evaluating the above effective magnetic moment,[34]

$$\mu_{eff}=g\mu_B\sqrt{J(J+1)}. \tag{2}$$

The giant magnetic moment of $6.1\mu_B$/Co obtained in Co-doped ZnO thin films is in close proximity to the calculated value of $6.6\mu_B$/Co. In contrast, the net spin moment calculated from spin-only formula $\mu_{eff}=g\mu_B\sqrt{S(S+1)}$ is $3.9\mu_B$, which is much lower than the experimental value.

As a large BMP in our $Zn_{0.96}Co_{0.04}O$ system, the hydrogenic orbital tends to sufficiently spread out to overlap with a large number of BMP, which makes few isolated polaron exist in our system be possible to perform supercoupling interaction. Only this condition is met, the giant magnetic moment of $6.1\mu_B$/Co in our case, which is slightly lower than effective magnetic moment $6.6\mu_B$/Co, can become reality. These interactions in an insulating state follow essentially from the Loss and DiVincenzo[35] proposal for spin-based solid-state quantum computing electrons localized in electrostatically defined quantum dots, with coupling between electron spins via the exchange interaction. In contrast, more remote impurities are interacting too weakly with both polarons to be of any importance. This is carried out in our lower-doped samples, e.g., (1 at. %) Co:ZnO, which produce much lower magnetic moments for weak interaction. On the other hand, for higher Co-doped films, an increase in the dopant concentration, i.e., (10 at. %) Co:ZnO, has been found to cause a rapid decrease in the moment due to enhanced dopant-dopant associations leading to progressive orbital moment quenching.[23,33] Also, in this case, antiferromagnetism or ferrimagnetism appears where there are continuous paths throughout the crystal joining nearest-neighbor magnetic cations.[24] The decreased moment observed in our higher Co-doped samples, and the drop in the moment after a high-temperature treatment (T_C measurement) in the low Co-doped sample, possibly caused by enhanced associations, suggest that the state may be similar in our case.

Based on BMP theory, T_C of dilute ferromagnetic oxides is given by[24]

$$T_C=[(S+1)s^2x\delta/3]^{1/2}J_{ij}f_O(r_c^{eff}/r_O)^3/k_B, \tag{3}$$

where S is a localized core spin, s is a donor electron of spin, x is doping concentration, δ is the donor concentration, J_{ij} is the s-d exchange parameter, f_0 is the oxygen packing fraction for the oxide, r_c^{eff} is the effective cation radius, k_B is Boltzmann's parameter. T_C can be estimated in the present case: $S=3/2$, $s=1/2$, $x=0.04$, $J_{ij}=3.6$ eV,[12] $\delta=0.01$, $r_c^{eff}=0.20$ nm, $r_0=0.14$ nm.[24] The T_C given by Eq. (3) is then roughly estimated to be 822 K, which is in the vicinity of the experimental results of 790 K. To some extent the calculation can explain the presence of high Curie temperature in the (4 at. %) Co:ZnO insulator. While the supercoupling mechanism claimed here remains speculative, the description it affords for the results appear reasonable, and efforts to pursue these processes further appear warranted.

IV. CONCLUSION

In summary, we have observed high-temperature ferromagnetism ($T_C\sim 790$ K) and giant magnetic moment ($6.1\mu_B$/Co) in Co-doped ZnO insulators. Co substituting for the Zn site of the 2+ charge state is uniform overall in the films. The combination of film growth by a certain amount of cobalt doping (~4 at. %) and low growth temperature deposition is proved to be key in enhancing the ferromagnetism of Co-doped ZnO. Such a capacity to produce a giant magnetic moment at the atomic level in dilute magnetic insulators make such dielectric films potentially useful in fabricating a wide range of components for spintronics, components for novel magnetic optical devices, and room temperature solid-state qubits.

ACKNOWLEDGMENTS

The authors are grateful for the financial support from the National Natural Science Foundation of China (Grant Nos. 50325105 and 50371040). Assistance from the TEM Lab and the Analysis Center of Tsinghua University is also acknowledged.

*Author to whom correspondence should be addressed. Electronic address: panf@mail.tsinghua.edu.cn

[1] L. Esaki, P. J. Stiles, and S. von Molnar, Phys. Rev. Lett. **19**, 852 (1967).
[2] J. M. Kikkawa and D. D. Awschalom, Nature (London) **397**, 139 (1999).
[3] M. Paillard, X. Marie, P. Renucci, T. Amand, A. Jbeli, and J. M. Gérard, Phys. Rev. Lett. **86**, 1634 (2001).
[4] S. A. Wolf, D. D. Awschalom, R. A. Buhrman, J. M. Daughton, S. von Molnár, M. L. Roukes, A. Y. Chtchelkanova, and D. M. Treger, Science **294**, 1488 (2001).
[5] K. A. Griffin, A. B. Pakhomov, C. M. Wang, S. M. Heald, and Kannan M. Krishnan, Phys. Rev. Lett. **94**, 157204 (2005).
[6] T. Zhao, S. R. Shinde, S. B. Ogale, H. Zheng, T. Venkatesan, R. Ramesh, and S. Das Sarma, Phys. Rev. Lett. **94**, 126601 (2005).
[7] T. Droubay, S. M. Heald, V. Shutthanandan, S. Thevuthasan, and S. A. Chambers, J. Appl. Phys. **97**, 046103 (2005).
[8] A. Kaminski and S. Das Sarma, Phys. Rev. Lett. **88**, 247202 (2002).
[9] J. M. D. Coey, A. P. Douvalis, C. B. Fitzgerald, and M. Venkatesan, Appl. Phys. Lett. **84**, 1332 (2004).
[10] A. H. Macdonald, P. Schiffer, and N. Samarth, Nat. Mater. **4**, 195 (2005).
[11] T. Dietl, H. Ohno, F. Matsukura, J. Cibert, and D. Ferrand, Science **287**, 1019 (2000).
[12] S. J. Pearton, C. R. Abernathy, M. E. Overberg, G. T. Thaler, D. P. Norton, N. Theodoropoulou, A. F. Hebard, Y. D. Park, F. Ren, J. Kim, and L. A. Boatner, J. Appl. Phys. **93**, 1 (2003).
[13] W. Prellier, A. Fouchet, and B. Mercey, J. Phys.: Condens. Matter **15**, R1583 (2003).
[14] K. Ueda, H. Tabata, and T. Kawai, Appl. Phys. Lett. **79**, 988 (2001).
[15] P. Sharma, A. Gupta, K. V. Rao, Frank J. Owens, R. Sharma, R. Ahuja, J. M. Osorio Guillen, B. Johansson, and G. A. Gehring, Nat. Mater. **2**, 673 (2003).
[16] T. Fukumura, Z. Jin, M. Kawasaki, T. Shono, T. Hasegawa, S. Koshihara, and H. Koinuma, Appl. Phys. Lett. **78**, 958 (2001).
[17] K. Ando, H. Saito, Z. Jin, T. Fukumara, M. Kawasaki, Y. Matsumoto, and H. Koinuma, J. Appl. Phys. **89**, 7284 (2001).
[18] A. C. Tuan, J. D. Bryan, A. B. Pakhomov, V. Shutthanandan, S. Thevuthasan, D. E. McCready, D. Gaspar, M. H. Engelhard, J. W. Rogers, Jr., K. Krishnan, D. R. Gamelin, and S. A. Chambers, Phys. Rev. B **70**, 054424 (2004).
[19] Z. Jin, M. Murakami, T. Fukumura, Y. Matsumoto, A. Ohtomo, M. Kawasaki, and H. Koinuma, J. Cryst. Growth **214/215**, 55 (2000).
[20] S. A. Chambers, S. M. Heald, and T. Droubay, Phys. Rev. B **67**, 100401(R) (2003).
[21] J. M. Berg, K. O. Hodgson, S. P. Cramer, J. L. Corbin, A. Elsberry, N. Pariyadath, and E. I. Stiefel, J. Am. Chem. Soc. **101**, 2774 (1979).
[22] F. Yang, T. He, J. B. Chen, and F. Pan, J. Appl. Phys. **91**, 3114 (2002).
[23] S. B. Ogale, R. J. Choudhary, J. P. Buban, S. E. Lofland, S. R. Shinde, S. N. Kale, V. N. Kulkarni, J. Higgins, C. Lanci, J. R. Simpson, N. D. Browning, S. Das Sarma, H. D. Drew, R. L. Greene, and T. Venkatesan, Phys. Rev. Lett. **91**, 077205 (2003).
[24] J. M. D. Coey, M. Venkatesan, and C. B. Fitzgerald, Nat. Mater. **4**, 173 (2005).
[25] S. R. Shinde, S. B. Ogale, S. Das Sarma, J. R. Simpson, H. D. Drew, S. E. Lofland, C. Lanci, J. P. Buban, N. D. Browning, V. N. Kulkarni, J. Higgins, R. P. Sharma, R. L. Greene, and T. Venkatesan, Phys. Rev. B **67**, 115211 (2003).
[26] S. Das Sarma, E. H. Hwang, and A. Kaminski, Phys. Rev. B **67**, 155201 (2003).
[27] J. J. Chen, Y. Gao, F. Zeng, D. M. Li, and F. Pan, Appl. Surf. Sci. **223**, 318 (2004).
[28] H. Toyosaki, T. Fukumura, Y. Yamada, K. Nakajima, T. Chikyow, T. Hasegawa, H. Koinuma, and M. Kawasaki, Nat. Mater. **3**, 221 (2004).
[29] P. A. Cox, *Transition Metal Oxides* (Clarendon, Oxford, 1992).
[30] N. H. Hong, J. Sakai, W. Prellier, and A. Hassini, J. Phys.: Condens. Matter **17**, 1697 (2005).
[31] N. H. Hong, J. Sakai, and A. Hassini, Appl. Phys. Lett. **84**, 2602 (2004).
[32] P. A. Wolff, R. N. Bhatt, and A. C. Durst, J. Appl. Phys. **79**, 5196 (1996).
[33] K. W. Edmonds, C. Binns, S. H. Baker, S. C. Thornton, C. Norris, J. B. Goedkoop, M. Finazzi, and N. B. Brookes, Phys. Rev. B **60**, 472 (1999).
[34] C. Kittel, *Introduction to Solid State Physics* (Wiley, New York, 1996).
[35] D. Loss and D. P. DiVincenzo, Phys. Rev. A **57**, 120 (1998).